Advanced Powder Technology 26 (2015) 819–829

Contents lists available at ScienceDirect

Advanced Powder Technology

journal homepage: www.elsevier.com/locate/apt

Original Research Paper

Stagnation-point heat transfer of nanofluids toward stretching sheets with variable thermo-physical properties

H. Zargartalebi [a], M. Ghalambaz [b,*], A. Noghrehabadi [a], A. Chamkha [c]

[a] Department of Mechanical Engineering, Shahid Chamran University of Ahvaz, Ahvaz, Iran
[b] Department of Mechanical Engineering, Dezful Branch, Islamic Azad University, Dezful, Iran
[c] Mechanical Engineering Department, Prince Mohammad Bin Fahd University (PMU), P.O. Box 1664, Al-Khobar 31952, Saudi Arabia

ARTICLE INFO

Article history:
Received 31 August 2014
Received in revised form 7 January 2015
Accepted 13 February 2015
Available online 26 February 2015

Keywords:
Nanofluid
Drift-flux
Stretching sheet
Variable thermal conductivity

ABSTRACT

The objective of this study is to investigate stagnation-point flow of nanofluids over an isothermal stretching sheet. The volume fraction of nanoparticles at the sheet is assumed to be passively controlled. Furthermore, due to low volume fraction of nanoparticles and dilute nanofluid, the thermal conductivity and dynamic viscosity of the nanofluid are assumed to be linear functions of the volume fraction of nanoparticles. In order to study the effects of a plethora of parameters on the boundary layer flow and heat and mass transfer, a practical range of these parameters have been utilized. An accurate numerical solution of the governing equations based on the finite difference method is obtained and the effect of various physical parameters such as the Prandtl number, Lewis number, thermophoresis parameter, and the Brownian motion parameter on the thermal, hydrodynamic, and concentration boundary layers is evaluated. In order to examine the alteration of the thermal convective coefficient, a dimensionless heat transfer enhancement ratio parameter is introduced. The results show that the variation of different thermodynamic parameters induces substantial impression on the behavior of the nanoparticles distribution. For example, it is found that an increase in the value of the Lewis number leads to a decrease in the value of the non-dimensional nanoparticles volume fraction at the sheet, but it does not have any influence on the thermal and hydrodynamic boundary layers. Increasing the Prandtl number is predicted to decrease the thermal boundary layer thickness and the volume fraction of nanoparticles at the surface. In most instances, the heat transfer augments in the presence of nanoparticles.

1. Introduction

The stagnation flow over a stretching sheet has attracted considerable pursuit of many researchers due to its broad range of applications in technology and industry. Some of these applications include polymer extrusion in a melt-spinning process, glass fiber, wire drawing, and cooling of metallic sheets or electronic chips. Depending on the rate of cooling in the process, the specified features would be produced. Sakiadis [1] was one of the first researchers who worked on the boundary layer on solid surfaces, after that many studies have been conducted on flow of Newtonian and non-Newtonian fluids over linear and non-linear stretching sheets [2–5]. Due to the importance of heat transfer in some fluids such as water, grease, oil, which are poor conductors with respect to others, researchers have endeavored to enhance the thermal conductivity of such fluids. For this purpose, they manufactured nanofluids intelligently. In fact, a nanofluid is a new engineered fluid which is synthesized of solid nanoparticles in a conventional heat transfer liquid (base fluid). The experimental measurements of the thermo-physical properties of nanofluids reveal that incorporation of the nanoparticles leads to augmentation of the thermal conductivity and the dynamic viscosity of the mixture [6–9]. Currently, there are several excellent reviews on the practical and potential industrial applications of nanofluids [10–12].

As mentioned above, the dispersion of nanoparticles in a base fluid would augment the thermal conductivity of the nanofluid. Therefore, it is expected that the presence of nanoparticles increases the convective heat transfer. However, the nanoparticles in the base fluid also alter the other thermo-physical properties such as the dynamic viscosity, density, and the heat capacity. Accordingly, the addition of nanoparticles may cause an increase or a decrease of the heat transfer coefficient of a nanofluid with respect to the base fluid. In addition, there are several slip

* Corresponding author. Tel.: +98 916 644 2671.
E-mail address: m.ghalambaz@iaud.ac.ir (M. Ghalambaz).

http://dx.doi.org/10.1016/j.apt.2015.02.008

Nomenclature

(x, y)	Cartesian coordinates
D_B	Brownian diffusion coefficient (m^2/s)
D_T	thermophoretic diffusion coefficient (m^2/s)
f	rescaled nanoparticles volume fraction, nanoparticles concentration
h	convective heat transfer coefficient (J/m^2)
k	thermal conductivity (W/m K)
Le	Lewis number
N_b	Brownian motion parameter
N_c	variable thermal conductivity parameter
N_t	thermophoresis parameter
N_v	variable viscosity parameter
P	pressure (Pa)
Pr	Prandtl number
Re_x	local Reynolds number
S	dimensionless stream function
T	temperature (K)
u, v	x and y velocity components (m/s)

Greek symbols

(ρc)	heat capacity (J/m^3 K)
μ	viscosity (Pa s)
α	thermal diffusivity (m^2/s)
η	dimensionless distance
θ	dimensionless temperature
ν	kinematic viscosity
ρ	density (kg/m^3)
φ	nanoparticles volume fraction
ψ	stream function

Subscripts

∞	free stream
bf	the base fluid
drift-flux	the drift flux model
nf	nanofluid
p	nanoparticles
w	sheet, wall, surface

mechanisms, including Brownian motion and thermophoresis effects, which tend to move the nanoparticles in the base fluid. The slip velocity of nanoparticles would affect the concentration and the heat transfer in the boundary layer. Hence, a special attention to the fundamental analysis of convective boundary layer heat transfer of nanofluids is highly demanded.

Due to the fact that the concentration of nanofluids would not remain constant and nanoparticles may have a slip velocity relative to the base fluid [13–15], some researchers showed that the migration of nanoparticles could transfer energy and also influence the thermo-physical properties [14,16]. Buongiorno [14] investigated the forces which affect the nanoparticles in the nanofluid. Buongiorno [14] found that the Brownian motion and the thermophoretic effects are two considerable forces which cause the drift-flux (slip velocity) of nanoparticles in the base fluid. Buongiorno [14] proposed a model to evaluate the concentration gradient of nanoparticles in the convective heat transfer flows.

Utilizing Buongiorno's model [14], different aspects of the convective boundary layers of nanofluids over a flat plate have been analyzed. For example, Khan and Pop [17] have evaluated the boundary layer flow and heat transfer of nanofluids over a linear stretching sheet. Moreover, different aspects of a boundary layer flow and heat transfer of nanofluids over a stretching sheet have been analyzed by previous researchers. Noghrehabadi et al. [15] considered a partial slip velocity for the nanofluid at the sheet. Rana and Bhargava [18] studied the effect of a non-linear velocity of the sheet. Makinde and Aziz [19] as well as Noghrehabadi et al. [20] examined the effect of a convective boundary condition below the sheet. Noghrehabadi et al. [21] analyzed the magnetohydrodynamic (MHD) effects for the same problem. Mustafa et al. [22] studied the flow of a nanofluid near the stagnation point toward an isothermal stretching surface. Hamad and Ferdows [23] analyzed the effect of a porous medium on the stagnation-point toward an isothermal stretching surface.

In all of the mentioned studies [13–15,17,18–23,24], it was assumed that the concentration of nanoparticles at the surface is controlled actively. Therefore, there is a mass flux of nanoparticles through the surface, and hence, the Sherwood number is non-zero there. However, there is not any justification for how the concentration of nanoparticles can be controlled actively at the surface.

In the mentioned studies [13–15,17,18–23,24], it was assumed that the migration of nanoparticles in the boundary layer would carry significant amount of energy. However, in a very recent study by Behseresht et al. [24], it has been reported that the energy transfer because of the migration of nanoparticles in natural convection flows is not significant. They have reported that the range of non-dimensional parameters corresponding to nanofluids, adopted in the literature, is not in agreement with the practical range of these parameters. The same conclusion is applicable in the case of a boundary layer flow over stretching sheets. In all of the mentioned studies [13–15,17,18–23], the Brownian motion parameter and thermophoresis parameter are assumed much larger than their practical values. In the most of the previous studies, these parameters are adopted in the order of 10^{-1}; however, they should be in the order of 10^{-6} and lower. Such low values of these parameters diminish the contribution of nanoparticles in the heat transfer equation. However, the concentration boundary layer is related to the ratio of thermophoresis to the Brownian motion parameter and may remain significant. In addition, the previous studies [13–15,17,18–23,24] assumed that the thermal conductivity and the dynamic viscosity of nanofluids are solely functions of the ambient volume fraction of nanoparticles and that they can be assumed constant in the governing equations. Hence, the effect of the local volume fraction of nanoparticles on the thermal conductivity and the dynamic viscosity was completely neglected. This assumption in the case of nanofluids could be an inadequate assumption. Because the experiments show that even a very low volume fraction of nanoparticles can significantly affect the thermo-physical properties of nanofluid [25,26]. In fact, since a nanofluid is a dilute mixture of a base fluid and nanoparticles, any variation of the concentration of nanoparticles in the base fluid could be significant.

The aim of the present study is to evaluate a stagnation-point flow and boundary layer heat and mass transfer of nanofluids over a stretching sheet. A practical boundary condition, the zero mass flux of nanoparticles through the sheet, is adopted. The dynamic viscosity and the thermal conductivity of the nanofluid are considered as functions of the local volume fraction of nanoparticles. The governing partial differential equations are transformed into a set of ordinary differential equations using similarity variables. Adopting the practical range of non-dimensional parameters, the effect of the nanofluids parameters on the boundary layer flow, heat and mass transfer is theoretically analyzed.

2. Mathematical formulation

Consider a two-dimensional incompressible stagnation-point flow and heat transfer of a nanofluid over an impermeable and isothermal stretching horizontal sheet. A schematic diagram of the physical model is illustrated in Fig. 1. According to the previous study, accomplished by Buongiorno [14], the migration of nanoparticles in the nanofluid is affected by two forces namely, Brownian diffusion and thermophoresis effects. Due to the thermophoresis effect, the nanoparticles move from a high temperature point to a low one. In this case, the thermophoresis parameter causes the nanoparticles to move away from the sheet because it is assumed that the sheet is hot. On the other hand, the Brownian diffusion force causes the nanoparticles to move from a high concentration point to a low one. Therefore, due to the Brownian motion effect, the concentration of the nanoparticles in the base fluid becomes uniform. It is assumed that the nanofluid is a dilute mixture of nanoparticles ($\varphi < 3.0\%$) in a base fluid. The nanoparticles are assumed to be in local thermal equilibrium with the base fluid [14] and that there are neither heat generation nor chemical reaction in the boundary layer.

Based on the previous experimental studies [6,7,27], the thermal conductivity and the dynamic viscosity of nanofluids are affected by fluctuations of the volume fraction of nanoparticles. As such, in the present study, both the thermal conductivity and the dynamic viscosity are assumed to be linearly dependent on the volume fraction of nanoparticles.

Utilizing conventional boundary layer approximations, the governing equations for continuity, momentum, energy, and concentration for the nanofluid are expressed respectively as follows:

$$\frac{\partial u}{\partial x}+\frac{\partial v}{\partial y}=0 \tag{1}$$

$$\rho_{nf}\left(u\frac{\partial u}{\partial x}+v\frac{\partial u}{\partial y}\right)=-\frac{\partial p}{\partial x}+\frac{\partial}{\partial x}\left(\mu_{nf,\infty}\frac{\partial u}{\partial x}\right)+\frac{\partial}{\partial y}\left(\mu_{nf,\infty}\frac{\partial u}{\partial y}\right) \tag{2}$$

$$\rho_{nf}\left(u\frac{\partial v}{\partial x}+v\frac{\partial v}{\partial y}\right)=-\frac{\partial p}{\partial y}+\frac{\partial}{\partial x}\left(\mu_{nf,\infty}\frac{\partial v}{\partial x}\right)+\frac{\partial}{\partial y}\left(\mu_{nf,\infty}\frac{\partial v}{\partial y}\right) \tag{3}$$

$$u\frac{\partial T}{\partial x}+v\frac{\partial T}{\partial y}=\frac{1}{(\rho c)_{nf}}\left[\frac{\partial}{\partial x}\left(k_{nf,\infty}\frac{\partial T}{\partial x}\right)+\frac{\partial}{\partial y}\left(k_{nf,\infty}\frac{\partial T}{\partial y}\right)\right]+\tau\left[D_B\left(\frac{\partial\varphi}{\partial x}\frac{\partial T}{\partial x}+\frac{\partial\varphi}{\partial y}\frac{\partial T}{\partial y}\right)+\frac{D_T}{T_\infty}\left[\left(\frac{\partial T}{\partial x}\right)^2+\left(\frac{\partial T}{\partial y}\right)^2\right]\right] \tag{4}$$

$$u\frac{\partial\varphi}{\partial x}+v\frac{\partial\varphi}{\partial y}=D_B\left(\frac{\partial^2\varphi}{\partial x^2}+\frac{\partial^2\varphi}{\partial y^2}\right)+\frac{D_T}{T_\infty}\left(\frac{\partial^2 T}{\partial x^2}+\frac{\partial^2 T}{\partial y^2}\right) \tag{5}$$

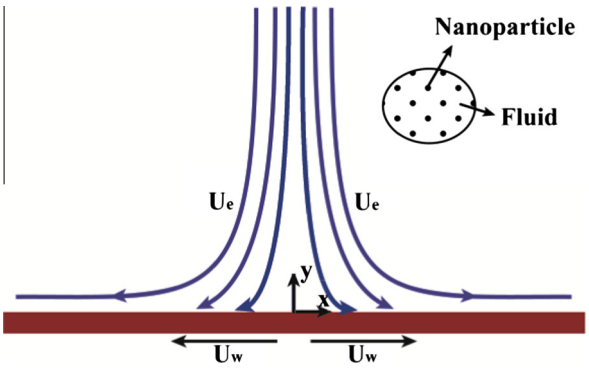

Fig. 1. Physical model and coordinate system.

where $\tau=(\rho c)_p/(\rho c)_{nf}$.

Subject to the relevant boundary conditions:

$$\begin{aligned} &u=u_w(x)=cx,\ v=0,\ T=T_w,\ D_B\tfrac{\partial\varphi}{\partial y}+\tfrac{D_T}{T_\infty}\tfrac{\partial T}{\partial y}=0 \quad \text{at } y=0\\ &u\to u_e(x)=ax,\ v\to 0,\ T\to T_\infty,\ \varphi\to\varphi_\infty \quad \text{as } y\to\infty \end{aligned} \tag{6}$$

in which the subscripts ∞ and w denote the ambient and surface conditions, respectively; u and v are the velocity components along the x and y directions, respectively; φ is the nanoparticles volume fraction, $k_{nf,\infty}$ is the thermal conductivity of the nanofluid, ρ_{nf} is the density of the nanofluid, D_B is the Brownian motion coefficient, and D_T is the thermophoretic diffusion coefficient. In essence, the no-slip boundary condition at $y=0$ is due to very low volume fraction of nanoparticles. As such, for high concentration of nanoparticles in which the particles do not properly stick at the surface the slip boundary condition should be considered. Moreover, It is worth noting that the zero mass flux of nanoparticles at the surface, i.e. $D_B(\partial\varphi/\partial y)+D_T/T_\infty(\partial T/\partial y)=0$, may result in negative values of nanoparticles volume fraction at the surface when the thermophoresis effect is the dominant force with respect to the Brownian motion force. Accordingly, the zero volume fraction of nanoparticles at the surface would be a substitute for the boundary condition in such cases as the negative volume fraction of nanoparticles is physically not valid.

Eqs. (1)–(5) could be easily reintroduced in a more simple form by expressing the following similar transformations:

$$\eta=\frac{y}{x}Re_x^{\frac{1}{2}},\quad S=\frac{\psi}{(U_{nf,\infty}\nu_{nf,\infty}x)^{\frac{1}{2}}},\quad \theta=\frac{T-T_\infty}{T_w-T_\infty},\quad f=\frac{\phi-\phi_\infty}{\phi_\infty} \tag{7}$$

in which η is the similarity variable, Re_x is the local Reynolds number defined as $Re_x=(\rho_{nf}U_{nf,\infty}x)/\mu_{nf,\infty}$, ψ is the stream function introduced as $u=\partial\psi/\partial y$ and $v=-\partial\psi/\partial x$, which satisfies the continuity equation. Using Eq. (7), Eqs.(1)–(5) are reduced to the nonlinear ordinary equations as follows (see Appendix A):

$$\left(\frac{\mu_{nf}(f)}{\mu_{nf,\infty}}\right)S'''+\left(\frac{\mu_{nf}(f)}{\mu_{nf,\infty}}\right)'S''+\frac{1}{2}SS''+1=0 \tag{8}$$

$$\left(\frac{k_{nf}(f)}{k_{nf,\infty}}\right)\theta''+\frac{1}{2}Pr_{nf}S\theta'+\left(\frac{k_{nf}(f)}{k_{nf,\infty}}\right)'\theta'+N_bf'\theta'+N_t\theta'^2=0 \tag{9}$$

$$f''+\frac{1}{2}Le\ Sf'+\frac{N_t}{N_b}\theta''=0 \tag{10}$$

subject to the dimensionless boundary conditions:

$$\begin{aligned} &S(0)=0,\quad S'(0)=\tfrac{c}{a},\quad \theta(0)=1,\quad N_bf'(0)+N_t\theta'(0)=0\\ &S'(\infty)\to 1,\quad \theta(\infty)\to 0,\quad f(\infty)\to 0 \end{aligned} \tag{11}$$

Here, the prime denotes ordinary derivative with respect to η, and the four non-dimensional parameters are defined by:

$$N_b=\frac{(\rho c)_pD_B\phi_\infty}{(\rho c)_{nf}\alpha_{nf,\infty}} \tag{12}$$

$$N_t=\frac{(\rho c)_pD_T(T_w-T_\infty)}{(\rho c)_{nf}\alpha_{nf,\infty}T_\infty} \tag{13}$$

$$Le=\frac{\nu_{nf,\infty}}{D_B} \tag{14}$$

$$Pr_{nf}=\frac{\nu_{nf,\infty}}{\alpha_{nf,\infty}} \tag{15}$$

The physical parameters, namely the local Nusselt number, Nu_x, and the skin friction coefficient Cf_x, are defined as follows:

$$Nu_x = \frac{h \cdot x}{k_{nf,\infty}} = \frac{q_W x}{k_{nf,\infty}(T_W - T_\infty)}. \tag{16}$$

$$Cf_x = \frac{\tau_{nf,w}}{\rho_f U_\infty^2} \tag{17}$$

where quantities of the surface heat flux q_w and the surface shear stress $\tau_{nf,w}$ are defined as follow:

$$q_w = -k_{nf,w}\left(\frac{\partial T}{\partial y}\right)_{y=0}, \quad \tau_{nf,w} = \mu_{nf,w}\left(\frac{\partial u}{\partial y}\right)_{y=0} \tag{18}$$

Substituting Eq. (18) into Eqs. (16), (17) and Using Eq. (7), the local Nusselt number and the skin friction coefficient are obtained as:

$$Nu_x\ Re_{nf,x}^{-\frac{1}{2}} = -\frac{k_{nf,w}}{k_{nf,\infty}}\theta'(0), \tag{19}$$

$$Cf_x\ Re_{nf,x}^{\frac{1}{2}} = \frac{\mu_{nf,w}}{\mu_{nf,\infty}} S''(0) \tag{20}$$

in which $Nu_x Re_{nf,x}^{-1/2}$ is the reduced Nusselt number, Nu_r.

As mentioned before, the thermal conductivity and the dynamic viscosity are considered to be linear functions of the nanoparticles' volume fraction, which are defined as:

$$\frac{k_{nf}}{k_{nf,\infty}} = 1 + N_c \frac{(\phi - \phi_\infty)}{\phi_\infty} \tag{21}$$

$$\frac{\mu_{nf}}{\mu_{nf,\infty}} = 1 + N_v \frac{(\phi - \phi_\infty)}{\phi_\infty} \tag{22}$$

where the coefficients N_c and N_v can be obtained using curve fitting of the available experimental data or analytical relations. It is worth noting that both the thermal conductivity and the dynamic viscosity depend linearly on the volume fraction only for $\varphi < 3.0\%$ and $\Delta T < 10$, otherwise these relationships would not be linear. Considering the two limits of zero volume fraction of nanoparticles at the surface ($\varphi_w = 0$ or $f(0) = -1$) and the free stream volume fraction of nanoparticles at the surface ($\varphi_w = \varphi_\infty$ or $f(0) = 0$), the values of N_c and N_v could be approximated as: $N_c = 1 - k_{bf}/k_{nf,\infty}$ and $N_v = 1 - \mu_{bf}/\mu_{nf,\infty}$. The earlier studies have widely utilized the Maxwell relation and the Brinkman model for calculating the thermal conductivity and dynamic viscosity of nanofluids, respectively [16,27]. Here, the validity of the linear function equations is checked with respect to the Maxwell and Brinkman models in Fig. 2. This figure depicts the ratios of $k_{nf}/k_{nf,\infty}$ and $\mu_{nf}/\mu_{nf,\infty}$ as functions of the local volume fraction of nanoparticles, evaluated using the present linear approximations as well as the analytical relations of Maxwell [7,28] and the Brinkman models [7,29]. These results show that there is an excellent agreement between the analytical models and the present linear approximations. Based on Fig. 2, it can be concluded that adjusting N_c and N_v can simulate the different models of the thermal conductivity and the dynamic viscosity. Therefore, Eqs. (21) and (22) are employed in this study for convenience. As a benchmark study, Buongiorno et al. [30] and Venerus et al. [31] have analyzed the effect of volume fraction of nanoparticles on the thermal conductivity and dynamic viscosity of nanofluids for different samples of nanofluids in 30 different laboratories around the world using different measurement methods. The results indicated that the thermal conductivity and dynamic viscosity of nanofluids are linear functions of the volume fraction of nanoparticles for low volume fractions of nanoparticles. Therefore, the linear function of concentration of particles for the thermal conductivity and viscosity is valid only in low concentrations of nanoparticles, and for high concentration of nanoparticles non-linear relations are required.

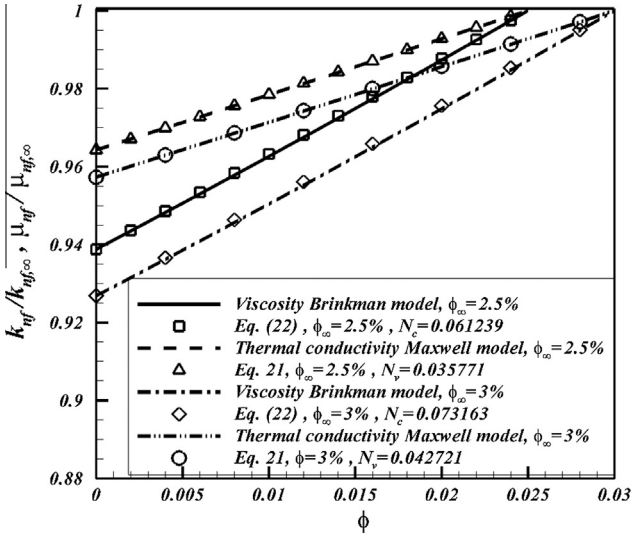

Fig. 2. Comparison between the evaluated values of local thermal conductivity and local viscosity of nanofluid as a function of local volume fraction of nanoparticles.

Substituting Eqs. (21) and (22) into Eqs. (19) and (20), respectively and using similar transportations, the reduced Nusselt number and the skin friction coefficient are expressed as follows:

$$Nur = -(1 + N_c \cdot f(0))\theta'_{nf}(0) \tag{23}$$

$$C_f\ Re_{\infty,x}^{\frac{1}{2}} = (1 + N_v \cdot f(0))S''(0) \tag{24}$$

For the purpose of investigating enhancement of heat transfer, due to the presence of nanoparticles in the base fluid, the following enhancement ratio is introduced as:

$$\frac{h_{drift-flux}}{h_{bf}} = (1 - N_v)^{\frac{1}{2}} \frac{1 + N_c \cdot f(0)}{1 - N_c} \frac{\theta'_{nf}(0)}{\theta'_{bf}(0)} \left(\frac{\rho_{nf}}{\rho_{bf}}\right)^{\frac{1}{2}} \tag{25}$$

The enhancement ratio represents the ratio of the convective heat transfer of the nanofluid to the convective heat transfer of the base fluid. The investigations showed that the reduced Nusselt number could not depict the enhancement of heat transfer owing to the presence of nanoparticles in the base fluid. In fact, using nanoparticles in the base fluid alters the values of the thermal conductivity, dynamic viscosity and other thermo-physical properties. For instance, the Reynolds numbers of the base fluid and the nanofluid are not identical. In other words, as shown, the dynamic viscosity of the nanofluid is higher than that of the base fluid. Therefore, the Reynolds number of the nanofluid could be lower than that of the base fluid. Accordingly, the heat transfer coefficient of the nanofluid, h_{nf}, could decline with respect to h_{bf}. Thereupon; the fluctuation of the reduced Nusselt number could not adequately show the enhancement of heat transfer due to the presence of nanoparticles in the base fluid. Despite the reduced Nusselt number, the alteration of both the thermal conductivity and the dynamic viscosity is considered in the enhancement ratio parameter ($h_{drif-flux}/h_{bf}$). Due to the fact that most of nanofluids are dilute mixtures of nanoparticles dispersed in base fluids, the magnitude of $(\rho_{nf}/\rho_{bf})^{1/2}$ is almost unity. As a case in point, in the case that Al_2O_3 nanoparticles are dispersed in water with a 2.5% volume fraction, the value of $(\rho_{nf}/\rho_{bf})^{1/2}$ is calculated to be equal to 1.018, which is roughly equal to unity. Therefore, this ratio could be removed from the relation, and consequently, Eq. (25) reduces to:

$$\frac{h_{drift-flux}}{h_{bf}} = (1 - N_v)^{\frac{1}{2}} \frac{1 + N_c \cdot f(0)}{1 - N_c} \frac{\theta'_{nf}(0)}{\theta'_{bf}(0)} \tag{26}$$

As the Prandtl numbers for the base fluid and the nanofluid are different, it is of interest to relate the Prandtl number of the nanofluid to the Prandtl number of the base fluid. Using Eq. (21) and (22), the Prandtl number of the nanofluid is a function of the Prandtl number of the base fluid, Pr_{bf}, as:

$$Pr_{nf} = Pr_{bf}\left(\frac{1-N_c}{1-N_v}\right)\times\frac{c_{nf}}{c_{bf}} \tag{27}$$

For a specified type of base fluid, the Prandtl number remains constant, and hence, the effect of addition of nanoparticles can be solely seen in the nanofluid parameters (N_v, N_c, N_b and N_t).

In fact, the ratio c_{nf}/c_{bf} is nearly unity. Since the nanofluid is assumed to be dilute, the value of c_{nf} is approximately equal to c_{bf}. For instance, the mentioned ratio for Alumina–water nanofluid with φ = 1% is 0.968 [32]. Hence, assuming this ratio to be unity is reasonable.

3. Results and discussion

Solving the set of Eqs. (8)–(10) numerically, the distributions of the velocity, temperature, and the volume fraction are obtained. Using the finite difference method with adjustable size of mesh and the 3-stage Lobatto IIIa formula with a collocation formula to uniform the error in the domain of the solution, the set of Eqs. (8)–(10) are solved. The details of the solution method can be found in [33]. In this method, η_∞ is replaced with a large value of 10 which is found to be adequate for proper approach of the physical variables to their free stream values. In order to validate the numerical method, the value of $S''(0)$, for a case in which a base fluid flows toward a stretching sheet, calculated in different a/c ratios and compared with similar investigations. Neglecting the Brownian motion and thermophoresis effects (i.e. $N_b = N_t = 0$) and assuming constant thermo-physical properties (i.e. $N_v = N_t = 0$), the present study reduces to the work of Ishak et al. [34] and Mahapatra and Gupta [35]. In this case, the calculations were executed for different values of η_∞ up to 40. An excellent agreement is noticed between the present study and the previous ones as shown in Table 1. It is clear that $\eta_\infty = 10$ is adequate for the numerical computations and therefore, is adopted for all calculations in the present study.

In order to study the effects of different parameters such as N_b, N_t, N_v, and N_c on the boundary layer flow and heat and mass transfer, a practical range of these parameters have been utilized. For water-based nanofluids which include nanoparticles of 100 nm diameters at room temperature, the Brownian diffusion coefficient, D_B, and the thermophoresis coefficient, D_T, are in the order of 10^{-11} [14,36,37]. As a case in point, a water base fluid filled with 100 nm of Al_2O_3 nanoparticles, the value of D_B and D_T are evaluated as 4.3948×10^{-11} and 9.946×10^{-11}, respectively. The Lewis number is in the range of $1\times10^{+3}$ to $5\times10^{+5}$. Furthermore, it is found that the values of N_b and N_t are very small and in the range of 1×10^{-8} to 1×10^{-4}. The constant parameters in the thermal conductivity and dynamic viscosity relations, e.g. N_c and N_v in Eqs. (21), (22), are usually in the range of 0–0.2 [38–42].

Table 1
Comparison of values of $S''(0)$ in different a/c ratios with the previous studies.

a/c	Mustafa et al. [22]	Ishak et al. [34]	Present		
			$\eta_\infty = 10$	$\eta_\infty = 20$	$\eta_\infty = 40$
0.01	−0.99823	−0.9980	−0.998028	−0.998024	−0.998024
0.1	−0.96954	−0.9694	−0.969386	−0.969386	−0.969386
0.2	−0.91813	−0.9181	−0.918107	−0.918107	−0.918107
0.5	−0.66735	−0.6673	−0.667263	−0.667263	−0.667263
2.0	2.01767	2.0175	2.017502	2.017502	2.017502
3.0	4.72964	4.7294	4.729282	4.729282	4.729282

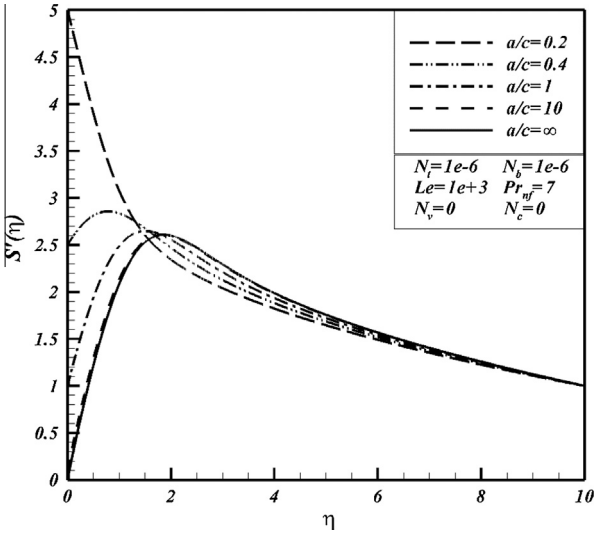

Fig. 3. The effect of a/c on velocity boundary layer.

The effects of the thermo-physical properties on the velocity, temperature, and the concentration boundary layers have been evaluated, considering all parameters to be fixed except one. The obtained representative results are presented and discussed below.

Firstly, the influence of the a/c ratio on the velocity boundary layer is examined in Fig. 3.

According to Fig. 3, the hydrodynamic boundary layer remains constant for the different ratios of a/c. As seen, despite the high values of the a/c ratio, the velocity values reduce in the vicinity of the sheet for low values of the a/c ratio. Since the ratio a/c represents the ratio of the free stream velocity to the velocity adjacent to the wall, augmentation of this ratio leads to reduction in the velocity near the wall. On the other hand, the effect of varying the ratio a/c becomes negligible for higher values of this proportion.

Fig. 4 shows the effect of the ratio a/c on the thermal boundary layer. As observed, an increase of the ratio a/c causes an increase the thermal boundary layer. In other words, when the ratio of a with respect to c grows, the free stream velocity becomes more vigorous toward the velocity adjacent to the wall, and consequently, $S'(0)\to 0$. Accordingly, based on the energy equations, the velocity values influence the temperature reciprocally; and hence, any reduction of velocity in the vicinity of the stretching sheet leads to thermal boundary layer augmentation.

The concentration boundary layer versus the dimensionless distance (η) for different a/c proportions is shown in Fig. 5. According to Fig. 3, increasing the ratio a/c leads to a drop in the value of the concentration at the surface. As mentioned, the augmentation of the ratio a/c reduces the velocity adjacent to the wall rather than free stream velocity. Therefore, in the low value of a/c, the nanoparticles gather in the vicinity of the sheet because the velocity near the wall is higher than the free stream velocity. In all cases, however, the non-dimensional concentration profiles, $f(\eta)$, at the surface are negative. The negative values of $f(\eta)$ indicate that the volume fraction of nanoparticles at the wall is lower than the free stream volume fraction of nanoparticles. Indeed, the reduction of the ratio a/c increases the concentration gradient. Accordingly, the Brownian motion effect goes up, and thereupon, the volume fraction of nanoparticles at the surface tends to the free stream volume fraction of nanoparticles, i.e. $f(0)$ diminishes.

In contrast, for high values of the ratio a/c, the nanoparticles distribute far from the wall and the number of these particles decreases at the surface. Moreover, it is revealed that the growth of the ratio a/c broadens the thickness of the concentration boundary layer significantly.

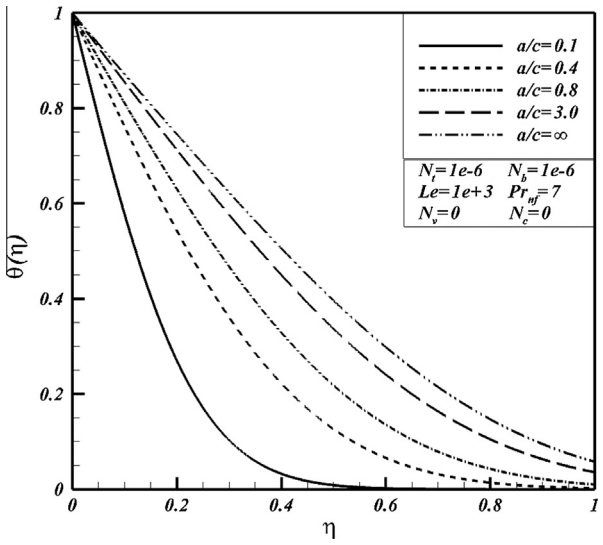

Fig. 4. The effect of a/c on thermal boundary layer.

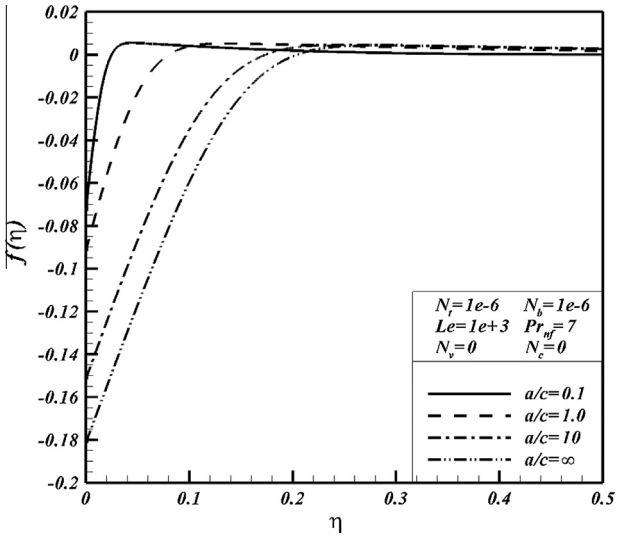

Fig. 5. The effect of a/c on concentration boundary layer.

In order to study the effect of the Lewis number on the nanoparticles' distribution, the concentration boundary layer for different Lewis numbers is shown in Fig. 6.

In accordance with Fig. 6, increasing the Lewis number tends to reduce the concentration boundary layer. As mentioned, the Lewis number is introduced as a proportion of the kinematic viscosity to the Brownian diffusion coefficient (D_B), as a consequence, an increase of the Lewis number means reducing the effect of D_B with respect to the kinematic viscosity. As the Lewis number decreases, the thickness of the concentration boundary layer becomes thin. On the other hand, far away from the surface and for low values of the Lewis number ($Le = 10^{+3}$), the dimensionless volume fraction of the nanofluid increases with respect to high values of the Lewis number state, and interestingly, the volume fraction of nanoparticles becomes more than the free stream volume fraction of nanoparticles. It is found that changes in the values of the Lewis number do not show any significant effects on the non-dimensional temperature and the velocity profiles. Hence, they have not been plotted for brevity.

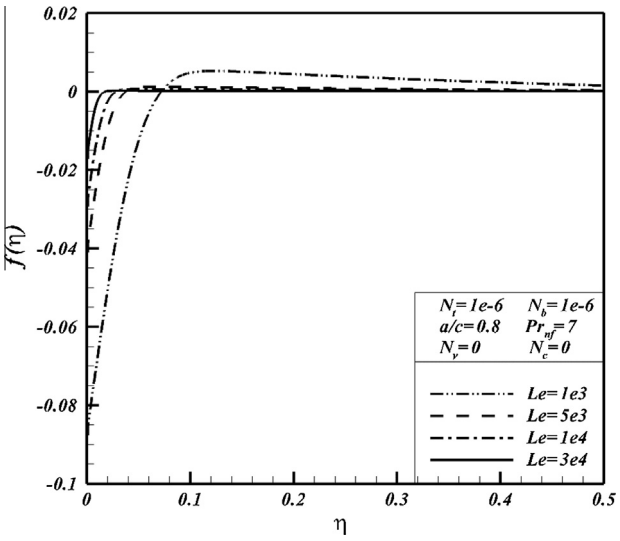

Fig. 6. The effect of Lewis number on concentration boundary layer.

The effect of variation of the Brownian parameter on the concentration boundary layer is depicted in Fig. 7. The presented results are categorized in two types. The first one is when the value of the Brownian number is low (e.g. $N_b \leqslant 10^{-8}$). In this case, the thermophoresis effect is the dominant effect and tends to induce negative volume fraction of nanoparticles at the surface ($f(0) < -1$). Hence, in order to be consistent with the physics (i.e. the negative volume fraction of nanoparticles is not possible), the volume fraction of the nanoparticles at the surface is set to zero. Indeed, when the value of the Brownian parameter is negligible with respect to the thermophoresis term, nanoparticles strongly move from a high temperature point (e.g. the sheet) to a low temperature point (e.g. far away from the sheet). It is clear that the nanoparticles which are swept from the surface are gathered in the vicinity of the sheet where the volume fraction of nanoparticles is higher than the free stream volume fraction ($f(\eta) > 0$). Therefore, the Brownian motion effect tends to disperse the nanoparticles toward the edge of the boundary layer. In the second behavior, whenever N_b becomes large, the value of the volume fraction increases at the sheet. For very high values of N_b, the volume

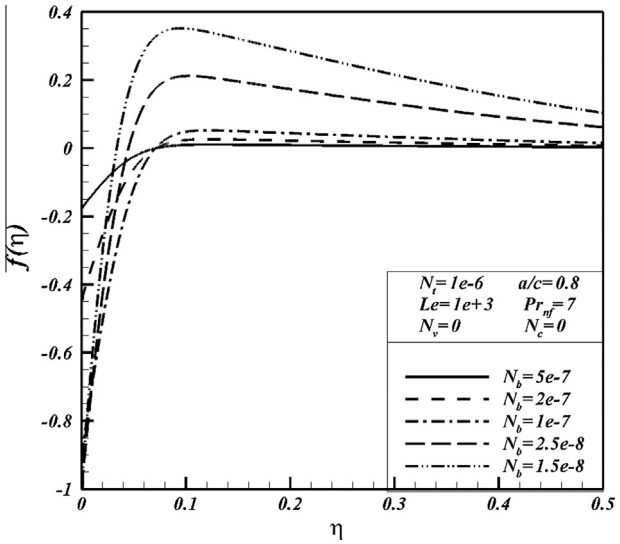

Fig. 7. The effect of Brownian motion on concentration boundary layer.

fraction of nanoparticles tends to reach the free stream volume fraction of nanoparticles. In the second behavior, the nanoparticles remain uniform and are approximately constant far from the sheet.

The effect of the thermophoresis parameter on the concentration boundary layer is presented in Fig. 8. As seen, increasing the value of N_t causes the volume fraction of nanoparticles at the surface to decline predictably. In addition, the concentration boundary layer thickness due to low values of N_t becomes thin. For instance, in the case where $N_t = 10^{-8}$, the width of the boundary layer is virtually vanished. The trend of results in this figure is in agreement with the results of Fig. 7.

It is worth noting that the variation of N_t and N_b do not have any considerable effect on the non-dimensional temperature and velocity profiles, and hence, they have not been plotted for brevity.

Afterwards, the effect of the Prandtl number on the dimensionless volume fraction of nanoparticles is investigated in Fig. 9. The Prandtl number is the ratio of the kinematic viscosity to the thermal diffusivity. In other words, the ratio of invariant hydrodynamic boundary layer to the thermal boundary layer. An augmentation of the Prandtl number would reduce the thickness of the thermal boundary layer. Thus, the temperature gradient in the vicinity of the sheet rises due to the reduction of the thermal boundary layer thickness. As the temperature gradient increases, the thermophoresis effect increases. This means that the nanoparticles move away from the sheet; and consequently, the value of the nanoparticles volume fraction diminishes. Furthermore, in the case in which $Pr_{nf} = 100$, the nanoparticles gather in a specific region ($0.08 < \eta < 0.15$) to compensate the low number of nanoparticles at the surface with respect to other conditions. This summit in the dimensionless volume fraction boundary layer appears owing to the constant number of nanoparticles in the fluid.

The influence of the Prandtl number on the thermal boundary layer is depicted in Fig. 10. The results show that the thermal boundary layer diminishes as a result of increasing the Prandtl number. Accordingly, the results are in good agreement with the previous results (Fig. 9). Notice that the hydrodynamic boundary layer remains relatively constant for various values of the Prandtl number. Therefore, the non-dimensional velocity profiles have not been presented.

Inspection of the governing equation of the conservation of nanoparticles, Eq. (10), shows that the boundary layer concentration of nanoparticles is directly related of the ratio of N_b/N_t. In addition, the direct contribution of these parameters in the energy

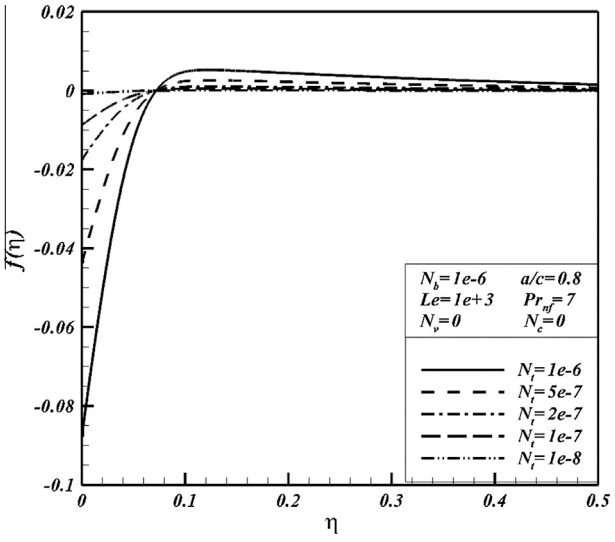

Fig. 8. The effect of thermophoresis parameter on concentration boundary layer.

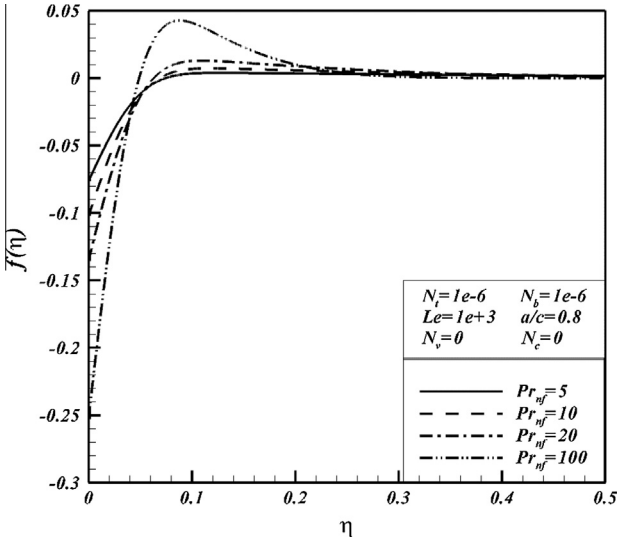

Fig. 9. The effect of Prandtl number on concentration boundary layer.

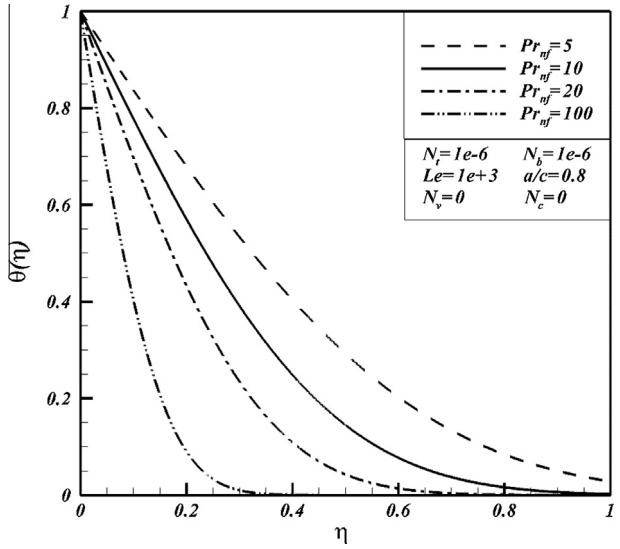

Fig. 10. The effect of Prandtl number on thermal boundary layer.

equation, Eq. (9), is negligible (because N_b and N_t are very small as they are in the order of 10^{-7} and lower). Therefore, it can be concluded that these parameters influence the concentration of nanoparticles in the boundary layer mainly through Eq. (10). Consequently, the local concentration of nanoparticles would affect the thermal conductivity and the dynamic viscosity of the nanofluid. Accordingly, the variation of the thermal conductivity and the dynamic viscosity would affect the velocity and temperature profiles and the heat transfer in the boundary layer. Therefore, the non-dimensional concentration profiles at the sheet are plotted versus the ratio N_b/N_t in Fig. 11. This figure shows the effect of variation of N_b/N_t on the values of $f(0)$ for selected values of the Lewis and Prandtl numbers. As seen, when the value of N_b with respect to N_t is negligible, the value of $f(0)$ remains constant, equals to -1. The increase of N_b/N_t results in the rise of $f(0)$. As discussed in Fig. 6, for high values of the Lewis number ($Le = 10^{+4}$), in which the Brownian effect becomes unimportant, the volume fraction of nanoparticles increases. In other words, regarding the cases for which $Pr_{nf} = 7$ and the Lewis numbers are 10^{+4} and 10^{+3}, the value of $f(0)$ arises in $N_b/N_t \approx 2 \times 10^{-2}$ and $N_b/N_t \approx 10^{-1}$ respectively. For

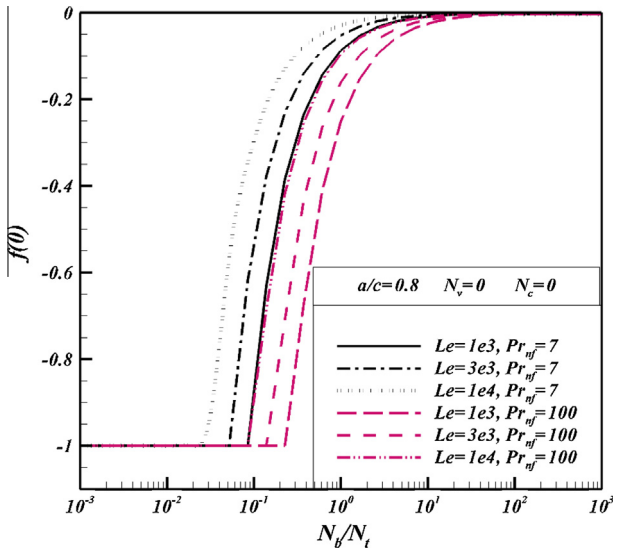

Fig. 11. The effect of Prandtl number, Lewis number, and N_b/N_t on concentration at the sheet.

instance, when $N_b/N_t = 3.16 \times 10^{-2}$, all the values of $f(0)$ are equal to -1 except for the case in which $Le = 10^{+4}$, $Pr = 7$ for which the value of $f(0)$ is -0.9287. Besides, the augmentation of the Prandtl number causes the nanoparticles to move away from the sheet. As a case in point, comparing the cases for which the Lewis number is 10^{+3} and the Prandtl numbers are 7 and 100, the magnitude of $f(0)$ increases in $N_b/N_t \approx 10^{-1}$ and $N_b/N_t \approx 2.1 \times 10^{-1}$, respectively.

Subsequently, the effects of the variable viscosity parameter (N_v) and the variable thermal conductivity parameter (N_c) are shown in Fig. 12. In order to depict the concentration profiles in the same range as the thermal boundary layer, the values of $f(\eta)$ have been multiplied by a constant value of -15 for convenience. As mentioned before, the Lewis number for nanofluids is very high and hence, the thickness of the concentration boundary is very low. Thus, a magnified view of the concentration profiles is provided in Fig. 12 to clearly show the concentration profiles in the vicinity of the sheet.

We have solved the governing equations for different combinations of non-dimensional parameters and the results show

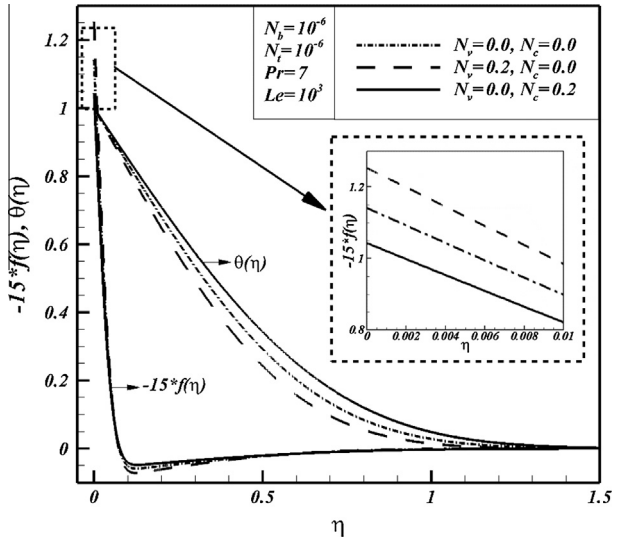

Fig. 12. The effect of N_v and N_c on concentration and thermal boundary layers.

that an increase in the value of N_c reduces the dimensionless temperature gradient. Therefore, this leads to a decline in the thermophoresis effect in the vicinity of the sheet. As such, the volume fraction of nanoparticles at the sheet increases. On the contrary, as the value of N_v increases, the dimensionless temperature gradient increases which means that the thermophoresis effect grows substantially. Consequently, the volume fraction of nanoparticles at the surface becomes lower. Moreover, when the magnitude of N_c increases, the thermal conductivity coefficient decreases, and therefore, the temperature gradient declines. Hence, the number of nanoparticles in the vicinity of the sheet, in the case which $N_c > N_v$, is higher than that in the case in which $N_c < N_v$. It is worth noting that the variation of both N_v and N_c has insignificant impression on the hydrodynamic boundary layer.

The non-dimensional parameters h_{drift_flux}/h_{bf}, Nu_r, and $S''_{nf}(0)/S''_{bf}(0)$ are illustrated in Tables 2–4, respectively for a practical range of N_v, N_c, Pr_b, and a/c. The values of the Brownian motion parameter, thermophoresis parameter, and the Lewis number are considered to be fixed as $N_b = 10^{-6}$, $N_t = 10^{-6}$, and $Le = 10^{+3}$.

It is clear that the variations of the Prandtl number and the ratio a/c do not have any effect on the enhancement ratio when $N_v = N_c = 0$ (Table 2). This is because of the fact that the values of N_b and N_t are very low, and the thermal conductivity and the dynamic viscosity of the nanofluid are also equal to those of the base fluid. Hence, it is expected that the enhancement ratio remains constant and equals to unity for different values of the Prandtl number and the ratio a/c. Nevertheless, owing to the fact that the enhancement ratio is a function of N_v, N_c, $f(0)$, and $\theta'_{nf}(0)/\theta'_{bf}(0)$, the variation of different parameters such as Pr_b, a/c, etc., changes the values of $f(0)$ and $\theta'_{nf}(0)/\theta'_{bf}(0)$ simultaneously. Hence, comparatively, depending on the set of parameters, the value of enhancement ratio alters erratically, but it is almost greater than unity which represents augmentation of heat transfer. Notwithstanding, it could be seen that an increase of N_c causes the value of the heat transfer enhancement ratio for every value of N_v. As it can be seen in some cases, the convective coefficient (h_{drift_flux}) increases about 13.49% (when $N_v = 0.1$, $N_c = 0.2$, $a/c = 10$, $Pr_b = 5$) and in some other cases, it reduces about -2.84% (when $N_v = 0.2$, $N_c = 0$, $a/c = 10$, $Pr_b = 5$). Therefore, it is clear that adjusting the nanofluid parameters would significantly enhance the heat transfer rate from the surface. However, non-adjustment of the nanofluid parameters would aggravate the heat transfer rate.

According to the results of Table 3, an increase in the Prandtl number leads to augmentation of the reduced Nusselt number. In fact, as mentioned before, increasing the Prandtl number tends to increase the non-dimensional temperature gradient and decreases $f(0)$. Obviously, a decrease in the value of $f(0)$ leads to a decrease in the magnitude of $k_{nf}(0)/k_{bf}(0)$, but, the results show that the rise of $\theta'_{nf}(0)$ is more effective than the reduction of $k_{nf}(0)/k_{bf}(0)$ for a fixed value of N_c. Furthermore, it could be seen that an increase in the value of N_c brings about a decrease in the value of the reduced Nusselt number. As previously mentioned, increasing the value of N_c leads to a rise in the number of nanoparticles at the sheet, and consequently, it is observed that the value of the thermal conductivity of the nanofluid reduces. On the other hand, it was stated that an increase in the value of N_c leads to a decrease in the non-dimensional temperature gradient. Thereupon, the reduced Nusselt number drops down. In addition, in accordance with Table 3, when the value of N_v goes up, the value of Nu_r soars similarly. In fact, the augmentation of N_v reduces the number of nanoparticles at the sheet; ergo, the value of thermal conductivity declines for a constant value of N_c. Besides, based on the explanations made regarding Fig. 10, it is found that a rise in the value of N_v brings about an increase in the dimensionless temperature gradient. As a result, it is evident that the increase of $\theta'_{nf}(0)$ is more influential than the decrease of $k_{nf}(0)/k_{bf}(0)$.

Table 2
The heat transfer enhancement ratio parameter h_{drift_flux}/h_{bf}.

N_v	N_c	$a/c = 0.1$			$a/c = 1.0$			$a/c = 10$		
		$Pr_b = 2$	$Pr_b = 5$	$Pr_b = 10$	$Pr_b = 2$	$Pr_b = 5$	$Pr_b = 10$	$Pr_b = 2$	$Pr_b = 5$	$Pr_b = 10$
0.0	0	1.0000	1.0000	1.0000	1.0000	1.0000	1.0000	1.0000	1.0000	1.0000
	0.05	1.0227	1.0239	1.0245	1.0292	1.0290	1.0286	1.0324	1.0327	1.0325
	0.1	1.0471	1.0497	1.0510	1.0609	1.0605	1.0596	1.0678	1.0683	1.0680
	0.15	1.0734	1.0777	1.0797	1.0955	1.0949	1.0936	1.1065	1.1074	1.1070
	0.2	1.1019	1.1081	1.1110	1.1334	1.1327	1.1309	1.1491	1.1505	1.1500
0.1	0	1.0062	1.0037	1.0025	0.9934	0.9938	0.9945	0.9869	0.9865	0.9867
	0.05	1.0292	1.0279	1.0271	1.0225	1.0226	1.0229	1.0190	1.0187	1.0187
	0.1	1.0540	1.0539	1.0538	1.0540	1.0539	1.0537	1.0540	1.0539	1.0537
	0.15	1.0807	1.0821	1.0827	1.0884	1.0880	1.0874	1.0922	1.0924	1.0921
	0.2	1.1096	1.1128	1.1141	1.1261	1.1255	1.1244	1.1343	1.1349	1.1344
0.2	0	1.0129	1.0076	1.0051	0.9862	0.9872	0.9887	0.9724	0.9716	0.9722
	0.05	1.0362	1.0320	1.0299	1.0150	1.0157	1.0168	1.0041	1.0033	1.0036
	0.1	1.0613	1.0583	1.0567	1.0463	1.0467	1.0473	1.0385	1.0379	1.0380
	0.15	1.0885	1.0867	1.0857	1.0804	1.0805	1.0807	1.0763	1.0758	1.0757
	0.2	1.1179	1.1177	1.1174	1.1178	1.1176	1.1173	1.1178	1.1176	1.1173

Table 3
The reduced Nusselt number $Nu_x Re_{nfx}^{-1/2}$.

N_v	N_c	$a/c = 0.1$			$a/c = 1.0$			$a/c = 10$		
		$Pr_b = 2$	$Pr_b = 5$	$Pr_b = 10$	$Pr_b = 2$	$Pr_b = 5$	$Pr_b = 10$	$Pr_b = 2$	$Pr_b = 5$	$Pr_b = 10$
0.0	0	2.2594	3.7331	5.3914	1.0320	1.5420	2.0966	0.8329	1.1659	1.4989
	0.05	2.1951	3.6314	5.2476	1.0091	1.5074	2.0487	0.8170	1.1438	1.4703
	0.1	2.1292	3.5271	5.1000	0.9854	1.4718	1.9995	0.8005	1.1211	1.4409
	0.15	2.0615	3.4198	4.9483	0.9610	1.4351	1.9490	0.7834	1.0975	1.4105
	0.2	1.9917	3.3094	4.7922	0.9358	1.3973	1.8968	0.7657	1.0731	1.3790
0.1	0	2.3965	3.9498	5.6972	1.0808	1.6155	2.1980	0.8665	1.2124	1.5591
	0.05	2.3288	3.8426	5.5456	1.0567	1.5791	2.1477	0.8500	1.1894	1.5292
	0.1	2.2592	3.7326	5.3900	1.0320	1.5418	2.0960	0.8329	1.1657	1.4984
	0.15	2.1878	3.6195	5.2301	1.0064	1.5033	2.0428	0.8152	1.1412	1.4667
	0.2	2.1142	3.5031	5.0656	0.9800	1.4636	1.9880	0.7968	1.1158	1.4340
0.2	0	2.5587	4.2058	6.0587	1.1380	1.7019	2.3176	0.9056	1.2665	1.6292
	0.05	2.4868	4.0921	5.8978	1.1127	1.6636	2.2643	0.8883	1.2425	1.5979
	0.1	2.4130	3.9755	5.7327	1.0866	1.6241	2.2096	0.8705	1.2177	1.5656
	0.15	2.3372	3.8556	5.5631	1.0597	1.5834	2.1533	0.8520	1.1920	1.5323
	0.2	2.2591	3.7321	5.3886	1.0319	1.5415	2.0953	0.8328	1.1655	1.4980

Table 4
The non-dimensional skin friction at the surface $S''_{nf}(0)/S''_{bf}(0)$.

N_v	N_c	$a/c = 0.1$			$a/c = 1.0$			$a/c = 10$		
		$Pr_b = 2$	$Pr_b = 5$	$Pr_b = 10$	$Pr_b = 2$	$Pr_b = 5$	$Pr_b = 10$	$Pr_b = 2$	$Pr_b = 5$	$Pr_b = 10$
0.1	0	1.0040	1.0065	1.0092	1.0057	1.0083	1.0111	1.0100	1.0138	1.0176
	0.05	1.0039	1.0064	1.0090	1.0055	1.0081	1.0108	1.0098	1.0136	1.0173
	0.1	1.0038	1.0062	1.0087	1.0054	1.0080	1.0106	1.0096	1.0134	1.0170
	0.15	1.0037	1.0060	1.0085	1.0053	1.0078	1.0104	1.0095	1.0132	1.0168
	0.2	1.0036	1.0058	1.0083	1.0052	1.0076	1.0102	1.0093	1.0129	1.0165
0.2	0	1.0086	1.0139	1.0196	1.0120	1.0176	1.0235	1.0210	1.0292	1.0372
	0.05	1.0084	1.0136	1.0192	1.0117	1.0172	1.0230	1.0207	1.0288	1.0367
	0.1	1.0082	1.0132	1.0187	1.0115	1.0169	1.0226	1.0203	1.0283	1.0361
	0.15	1.0079	1.0129	1.0182	1.0112	1.0165	1.0221	1.0199	1.0278	1.0355
	0.2	1.0077	1.0125	1.0177	1.0109	1.0161	1.0215	1.0195	1.0273	1.0348

It is seen that as the value of the ratio a/c increases, the reduced Nusselt number drops down. This is expected as it was shown previously that increasing the ratio a/c reduces both of the non-dimensional temperature gradient and the concentration at the surface. Consequently, the reduced Nusselt number declines.

According to the results of Table 4, it is seen that an increase in the value of N_c leads to a decrease in the non-dimensional velocity gradient at the surface. In fact, as mentioned before, the rise of N_c tends to increase $f(0)$. Therefore, based on the dynamic viscosity relation (Eq. (22)), the value of $\mu_{nf}(0)/\mu_{bf}(0)$ diminishes for a specified value of N_v; and as a consequence, increasing N_c tends to decrease $S''_{nf}(0)/S''_{bf}(0)$. Moreover, the results show that when the value of N_v soars up, the non-dimensional velocity gradient goes up consequently. As the value of N_v increases, the value of the concentration at the surface, $f(0)$, goes up. Hence, the dynamic viscosity, depending on the value of $N_v \times f(0)$, may increase or decrease. It is worth mentioning that, when $N_v = 0$, since the value of $\mu_{nf}(0)$ becomes equal to $\mu_{bf}(0)$, the value of $S''_{nf}(0)/S''_{bf}(0)$ is unity. In addition, a rise in the value of Pr_b leads to an increase in the value $S''_{nf}(0)/S''_{bf}(0)$. Generally, the value of the non-dimensional skin friction is higher than unity due to the presence of nanoparticles.

4. Conclusion

The stagnation-point flow of nanofluids toward an isothermal stretching sheet is analyzed. It is assumed that the sheet is impermeable and the mass flux of nanoparticles at the sheet is zero. The impact of different crucial parameters such as the Prandtl number, free stream to wall velocity ratio a/c, thermophoresis parameter, and the Brownian motion parameter, etc. on the thermal, concentration, and the hydrodynamic boundary layers is evaluated. Furthermore, on account of the local effect of nanoparticles in the base fluid, the thermal conductivity and the dynamic viscosity are imposed to be linear functions of the non-dimensional volume fraction of nanoparticles. The main results of the present study can be summarized as follows:

1. The variation of the ratio a/c does not influence the thickness of the hydrodynamic boundary layer. It is found that for high values of a/c, the variation of the hydrodynamic profile becomes negligible and independent of the ratio a/c. On the other hand, it is seen that as the value of the ratio a/c, the thermal boundary layer thickness increases and the volume fraction of nanoparticles at the stretching sheet drops down.
2. When the value of the Lewis number soars, the volume fraction of nanoparticles at the sheet declines. On the other hand, the results show that altering the Lewis number does not have substantial influence on the thermal and hydrodynamic boundary layers.
3. Changing the parameters N_b and N_t does not comparatively affect the non-dimensional temperature and velocity values. The non-dimensional volume fraction of nanoparticles at the sheet predictably rises when the values of N_b and N_t increase and decrease, respectively. It is found that the concentration boundary layer nearly vanishes for low values of N_t (e.g. $N_t = 10^{-8}$).
4. Changing the Prandtl number has inconsiderable impact on the hydrodynamic boundary layer. Nevertheless, the thickness of thermal boundary layer becomes thin for high values of the Prandtl number. It means that the non-dimensional temperature gradient increases in this state; and therefore, the thermophoresis effect goes up and brings about a reduction in the volume fraction of nanoparticles at the surface.
5. The magnitudes of the important dimensionless parameters, namely h_{drift_flux}/h_{bf}, Nu_r, and $S''_{nf}(0)/S''_{bf}(0)$, are evaluated for different values of non-dimensional parameters namely the Prandtl number, a/c, N_c, and N_v. It is found that in most instances, h_{drift_flux}/h_{bf} is higher than unity, and consequently, the heat transfer augments in the presence of nanoparticles. The fluctuation of the non-dimensional parameters N_v, N_c, Pr_b, and a/c, is found to influence the non-dimensional skin friction slightly. It is also found that the non-dimensional skin friction is higher than unity in all cases.

Acknowledgement

The third author is grateful to Shahid Chamran University of Ahvaz for its crucial support. The second author is grateful to Dezful Branch, Islamic Azad University for its support. Noghrehabadi, Zargartalebi and Ghalambaz acknowledge the Iran Nanotechnology Initiative Council (INIC) for financial support.

Appendix A

Using the boundary layer approximations, the momentum equations, Eq. (2), is written as:

$$\rho_{nf}\left(u\frac{\partial u}{\partial x}+v\frac{\partial u}{\partial y}\right)=-U_e\frac{dU_e}{dx}+\frac{\partial\left(\mu_{nf}(\phi)\frac{\partial u}{\partial y}\right)}{\partial y} \tag{A1}$$

which can be rewritten as:

$$\rho_{nf}\left(u\frac{\partial u}{\partial x}+v\frac{\partial u}{\partial y}\right)=-U_e\frac{dU_e}{dx}+\frac{\partial\frac{\mu_{nf}(\phi)}{\mu_{nf,\infty}}}{\partial y}\frac{\partial u}{\partial y}+\frac{\mu_{nf}(\phi)}{\mu_{nf,\infty}}\frac{\partial\left(\frac{\partial u}{\partial y}\right)}{\partial y} \tag{A2}$$

where using similarity variables:

$$\frac{\partial\eta}{\partial y}=\frac{Re_x^{\frac{1}{2}}}{x},\quad\text{and}\quad\frac{\partial\eta}{\partial x}=-\frac{1}{2}\frac{\eta}{x}, \tag{A3}$$

$$v=v_{nf}\frac{1}{2}\frac{Re_x^{\frac{1}{2}}}{x}(\eta S'-S) \tag{A4}$$

$$u=U_\infty S' \tag{A5}$$

The other terms of Eq. (A2) have been obtained as:

$$\frac{\partial u}{\partial x}=\frac{\partial u}{\partial S'}\frac{\partial S'}{\partial\eta}\frac{\partial\eta}{\partial x}=-\frac{1}{2}\frac{\eta}{x}U_\infty S'' \tag{A6}$$

$$\frac{\partial u}{\partial y}=\frac{\partial u}{\partial S'}\frac{\partial S'}{\partial\eta}\frac{\partial\eta}{\partial y}=\frac{Re_x^{\frac{1}{2}}}{x}U_\infty S'' \tag{A7}$$

$$\frac{\partial^2 u}{\partial y^2}=\frac{\partial u}{\partial S''}\frac{\partial S''}{\partial\eta}\frac{\partial\eta}{\partial y}=U_\infty\frac{Re_x}{x^2}S''' \tag{A8}$$

$$\frac{\partial\frac{\mu_{nf}(\phi)}{\mu_{nf,\infty}}}{\partial y}=\frac{\partial\eta}{\partial y}\frac{\partial\left(\frac{\mu_{nf}(\phi_\infty f+\phi_\infty)}{\mu_{nf,\infty}}\right)}{\partial\eta} \tag{A9}$$

Substituting Eqs. (A4)–(A9) in Eq. (A2) yields:

$$\begin{aligned}\rho_{nf}&\left(-\frac{1}{2}\frac{\eta}{x}U_\infty S''U_\infty S'+v_{nf}\frac{1}{2}\frac{Re_x^{\frac{1}{2}}}{x}(\eta S'-S)\frac{Re_x^{\frac{1}{2}}}{x}U_\infty S''\right)\\&=ax^2+\frac{Re_x^{\frac{1}{2}}}{x}\frac{\partial[v_{nf}(\phi_\infty f+\phi_\infty)]}{\partial\eta}\frac{Re_x^{\frac{1}{2}}}{x}U_\infty S''+v_{nf}(\phi_\infty f\\&\quad+\phi_\infty)U_\infty\frac{Re_x}{x^2}S'''\end{aligned} \tag{A10}$$

Simplifying Eq. (A10) leads to Eq. (8).

Using typical boundary layer assumptions, Eq. (3), in the Cartesian system, is written as:

$$\begin{aligned}(\rho c)_{nf}\left(u\frac{\partial T}{\partial x}+v\frac{\partial T}{\partial y}\right)&=k_{nf,\infty}\frac{\partial\left(\frac{k_{nf}(\phi)}{k_{nf,\infty}}\right)}{\partial y}\frac{\partial T}{\partial y}+k_{nf,\infty}\left(\frac{k_{nf}(\phi)}{k_{nf,\infty}}\right)\frac{\partial^2 T}{\partial y^2}\\&\quad+(\rho c)_p\left[D_B\frac{\partial\varphi}{\partial y}\frac{\partial T}{\partial y}+\frac{D_T}{T_\infty}\left(\frac{\partial T}{\partial y}\right)^2\right]\end{aligned} \tag{A11}$$

where:

$$\frac{\partial T}{\partial y}=\frac{\partial T}{\partial\theta}\frac{\partial\theta}{\partial\eta}\frac{\partial\eta}{\partial y}=(T_w-T_\infty)\theta'\frac{Re_x^{\frac{1}{2}}}{x} \tag{A12}$$

$$\frac{\partial\phi}{\partial y}=\frac{\partial\phi}{\partial f}\frac{\partial f}{\partial\eta}\frac{\partial\eta}{\partial y}=\phi_\infty f'\frac{Re_x^{\frac{1}{2}}}{x} \tag{A13}$$

$$\frac{\partial T}{\partial x}=\frac{\partial T}{\partial\theta}\frac{\partial\theta}{\partial\eta}\frac{\partial\eta}{\partial x}=-\frac{1}{2}(T_w-T_\infty)\frac{\eta}{x}\theta' \tag{A14}$$

$$\frac{\partial^2 T}{\partial y^2}=\frac{\partial T}{\partial\theta'}\frac{\partial\theta'}{\partial\eta}\frac{\partial\eta}{\partial y}=(T_w-T_\infty)\frac{Re_x}{x^2}\theta'' \tag{A15}$$

$$\frac{\partial\frac{k_{nf}(\phi)}{k_{nf,\infty}}}{\partial y}=\frac{\partial\eta}{\partial y}\frac{\partial\left(\frac{k_{nf}(\phi_\infty f+\phi_\infty)}{k_{nf,\infty}}\right)}{\partial\eta} \tag{A16}$$

Substituting Eqs. (A4)–(A7) and Eqs. (A12)–(A16) into Eq. (A10) yields:

$$-\frac{1}{2}\frac{\eta}{x}(T_w-T_\infty)\theta' U_\infty S'+\frac{1}{2}v_{nf}\frac{Re_x^{\frac{1}{2}}}{x}(\eta S'-S)(T_w-T_\infty)\theta'\frac{Re_x^{\frac{1}{2}}}{x}$$
$$=\frac{k_{nf,\infty}}{(\rho c)_{nf}}\frac{Re_x^{\frac{1}{2}}}{x}\frac{\partial\left(\frac{k_{nf}(\varphi_\infty f+\varphi_\infty)}{k_{nf,\infty}}\right)}{\partial\eta}(T_w-T_\infty)\frac{Re_x^{\frac{1}{2}}}{x}\theta'$$
$$+\frac{k_{nf,\infty}}{(\rho c)_{nf}}\frac{k_{nf}(\varphi_\infty f+\varphi_\infty)}{k_{nf,\infty}}(T_w-T_\infty)\frac{Re_x}{x^2}\theta''$$
$$+\frac{(\rho c)_p}{(\rho c)_{nf}}\left[D_B\phi_\infty f'\frac{Re_x}{x^2}(T_w-T_\infty)\theta'+\frac{D_T}{T_\infty}\frac{Re_x}{x^2}(T_w-T_\infty)^2\theta'^2\right] \quad (A17)$$

Simplifying Eq. (A17) leads to Eq. (9).

The conservation of nanoparticles, Eq. (4), is written as:

$$\left[u\frac{\partial\phi}{\partial x}+v\frac{\partial\phi}{\partial y}\right]=D_B\frac{\partial^2\phi}{\partial y^2}+\left(\frac{D_T}{T_\infty}\right)\frac{\partial^2 T}{\partial y^2} \quad (A18)$$

where

$$\frac{\partial\phi}{\partial x}=\frac{\partial\phi}{\partial f}\frac{\partial f}{\partial\eta}\frac{\partial\eta}{\partial x}=-\frac{1}{2}\frac{\eta}{x}\phi_\infty f' \quad (A19)$$

$$\frac{\partial^2\phi}{\partial y^2}=\frac{\partial\phi}{\partial f'}\frac{\partial f'}{\partial\eta}\frac{\partial\eta}{\partial y}=\phi_\infty f''\frac{Re_x}{x^2} \quad (A20)$$

Substituting Eqs. (A4), (A5), (A13), (A15), (A19) and (A20) into Eq. (A18) yields:

$$-\frac{1}{2}\frac{\eta}{x}\phi_\infty f' U_\infty S'+\frac{1}{2}v_{nf}\frac{Re_x^{\frac{1}{2}}}{x}(\eta S'-S)\phi_\infty f'\frac{Re_x^{\frac{1}{2}}}{x}=D_B\phi_\infty f''\frac{Re_x}{x^2}+\left(\frac{D_T}{T_\infty}\right)(T_w-T_\infty)\frac{Re_x}{x^2}\theta'' \quad (A21)$$

Simplifying Eq. (A21) leads to Eq. (A10).

Using Eqs. (21) and (22), the terms $\frac{\mu_{nf}(f)}{\mu_\infty}$, $\left(\frac{\mu_{nf}(f)}{\mu_\infty}\right)'$, $\frac{k_{nf}(f)}{k_\infty}$ and $\left(\frac{k_{nf}(f)}{k_\infty}\right)'$ are obtained as $\frac{k_{nf}}{k_{nf,\infty}}=1+N_c\cdot f$, $\left(\frac{k_{nf}}{k_{nf,\infty}}\right)'=N_c\cdot f'$, $\frac{\mu_{nf}}{\mu_{nf,\infty}}=1+N_v\cdot f$ and $\left(\frac{\mu_{nf}}{\mu_{nf,\infty}}\right)'=N_v\cdot f'$.

References

[1] B.C. Sakiadis, Boundary layer behavior on continuous solid surfaces: I Boundary layer equations for two dimensional and axisymmetric flow, AIChE J. 7 (1961) 26–28.
[2] S.K. Khan, M. Subhas Abel, M. Sonth Ravi, Viscoelastic MHD flow heat and mass transfer over a porous stretching sheet with dissipation of energy and stress work, Int. J. Heat Mass Transf. 40 (2003) 47–57.
[3] N. Bachok, A. Ishak, R. Nazar, Flow and heat transfer over an unsteady stretching sheet in a micropolar fluid with prescribed surface heat flux, Int. J. Math. Mod. Meth. Appl. Sci. 4 (2010) 167–176.
[4] N. Bachok, A. Ishak, I. Pop, On the stagnation point flow towards a stretching sheet with homogeneous–heterogeneous reactions effects, Commun. Nonlinear Sci. Numer. Simulat. 16 (2011) 4296–4302.
[5] N. Bachok, A. Ishak, R. Nazar, Flow and heat transfer over an unsteady stretching sheet in a micropolar fluid, Meccanica 46 (2011) 935–942.
[6] S. Kakaç, A. Pramuanjaroenkij, Review of convective heat transfer enhancement with nanofluids, Int. J. Heat Mass Transf. 52 (2009) 3187–3196.
[7] K. Khanafer, K. Vafai, A critical synthesis of thermophysical characteristics of nanofluids, Int. J. Heat Mass Transf. 54 (2011) 4410–4428.
[8] S.K. Das, S. Choi, W. Yu, T. Pradeep, Nanofluids: Science and Technology, Wiley Interscience, New Jersey, 2007.
[9] Choi SUS, Enhancing thermal conductivity of fluids with nanoparticle, in: D.A. Siginer, H.P. Wang (Eds.), Developments and Applications of Non-Newtonian Flows, ASME FED, 231/MD 66, 1995, pp. 99–105.
[10] R. Saidur, K.Y. Leong, H.A. Mohammad, A review on applications and challenges of nanofluids, Renew. Sustain. Energy Rev. 15 (2011) 1646–1668.
[11] G. Huminic, A. Humini, Application of nanofluids in heat exchangers: a review, Renew. Sustain. Energy Rev. 16 (2012) 5625–5638.
[12] L. Godson, B. Raja, D. Mohan Lal, S. Wongwises, Enhancement of heat transfer using nanofluids—an overview, Renew. Sustain. Energy Rev. 14 (2010) 629–641.
[13] N. Bachok, A. Ishak, I. Pop, Boundary-layer flow of nanofluids over a moving surface in a flowing fluid, Int. J. Therm. Sci. 49 (2010) 1663–1668.
[14] J. Buongiorno, Convective transport in nanofluids, J. Heat Transfer 128 (2006) 240–245.
[15] A. Noghrehabadi, R. Pourrajab, M. Ghalambaz, Effect of partial slip boundary condition on the flow and heat transfer of nanofluids past stretching sheet prescribed constant wall temperature, Int. J. Therm. Sci. 54 (2012) 253–261.
[16] N.A. Yacob, A. Ishak, R. Nazar, I. Pop, Falkner-Skan problem for a static and moving wedge with prescribed surface heat flux in a nanofluid, Int. Commun. Heat Mass Transfer 38 (2011) 149–153.
[17] W.A. Khan, I. Pop, Boundary-layer flow of a nanofluid past a stretching sheet, Int. J. Heat Mass Transf. 53 (2010) 2477–2483.
[18] P. Rana, R. Bhargava, Flow and heat transfer of a nanofluid over a nonlinearly stretching sheet: a numerical study, Commun. Nonlinear Sci. Numer. Simul. 17 (2012) 212–226.
[19] O.D. Makinde, A. Aziz, Boundary layer flow of a nanofluid past a stretching sheet with a convective boundary condition, Int. J. Therm. Sci. 50 (2011) 1326–1332.
[20] A. Noghrehabadi, R. Pourrajab, M. Ghalambaz, Flow and heat transfer of nanofluids over stretching sheet taking into account partial slip and thermal convective boundary conditions, Heat Mass Transf. 49 (2013) 1357–1366.
[21] A. Noghrehabadi, M. Ghalambaz, A. Ghanbarzadeh, Heat transfer of magnetohydrodynamic viscous nanofluids over an isothermal stretching sheet, J. Thermophys. Heat Transfer 26 (2012) 686–689.
[22] M. Mustafa, T. Hayat, I. Pop, S. Asghar, S. Obaidat, Stagnation-point flow of a nanofluid towards a stretching sheet, Int. J. Heat Mass Transf. 54 (2011) 5588–5594.
[23] M.A.A. Hamad, M. Ferdows, Similarity solution of boundary layer stagnation-point flow towards a heated porous stretching sheet saturated with a nanofluid with heat absorption/generation and suction/blowing: a Lie group analysis, Commun. Nonlinear Sci. Numer. Simul. 17 (2012) 132–140.
[24] A. Behseresht, A. Noghrehabadi, M. Ghalambaz, Natural-convection heat and mass transfer from a vertical cone in porous media filled with nanofluids using the practical ranges of nanofluids thermo-physical properties, Chem. Eng. Res. Des. 92 (2014) 447–452.
[25] L.S. Sundar, K.V. Sharma, M.T. Naik, M.K. Singh, Empirical and theoretical correlations on viscosity of nanofluids: a review, Renew. Sustain. Energy Rev. 25 (2013) 670–686.
[26] R.S. Vajjha, D.K. Das, A review and analysis on influence of temperature and concentration of nanofluids on thermophysical properties, heat transfer and pumping power, Int. J. Heat Mass Transf. 55 (2012) 4063–4078.
[27] N. Bachok, A. Ishak, I. Pop, Flow and heat transfer characteristics on a moving plate in a nanofluid, Int. J. Heat Mass Transf. 55 (2012) 642–648.
[28] J.C. Maxwell, A Treatise on Electricity and Magnetism, second ed., Clarendon Press, Oxford, UK, 1881.
[29] H.C. Brinkman, The viscosity of concentrated suspensions and solutions, J. Chem. Phys. 20 (1952) 571–581.
[30] J. Buongiorno, D.C. Venerus, N. Prabhat, T. McKrell, J. Townsend, R. Christianson, et al., A benchmark study on the thermal conductivity of nanofluids, J. Appl. Phys. 106 (2009) 094312.
[31] D.C. Venerus, J. Buongiorno, R. Christianson, J. Townsend, I.C. Bang, G. Chen, et al., Viscosity measurements on colloidal dispersions (nanofluids) for heat transfer applications, Appl. Rheol. 20 (2010) 44582.
[32] H.A. Mohammed, P. Gunnasegaran, N.H. Shuaib, Heat transfer in rectangular microchannels heat sink using nanofluids, Int. Commun. Heat Mass Transfer 37 (2010) 1496–1503.
[33] L.F. Shampine, J. Kierzenka, M.W. Reichelt, Solving Boundary Value Problems for Ordinary Differential Equations in MATLAB with bvp4c. Tutorial notes, 2000.
[34] A. Ishak, R. Nazar, N. Amin, D. Filip, I. Pop, Mixed convection in the stagnation point flow towards a stretching vertical permeable sheet, Malay. J. Math. Sci. 2 (2007) 217–226.
[35] T.R. Mahapatra, A.S. Gupta, Heat transfer in the stagnation-point flow towards a stretching surface, Heat Mass Transfer 38 (2002) 517–521.
[36] A. Behseresht, A. Noghrehabadi, M. Ghalambaz, Natural-convection heat and mass transfer from a vertical cone in porous media filled with nanofluids using the practical ranges of nanofluids thermo-physical properties, Chem. Eng. Res. Des. 92 (2014) 447–452.
[37] A. Noghrehabadi, M. Ghalambaz, A. Ghanbarzadeh, Effects of variable viscosity and thermal conductivity on natural-convection of nanofluids past a vertical plate in porous media, J. Mech. 30 (2014) 265–275.
[38] M. Chandrasekar, S. Suresh, Bose A. Chandra, Experimental investigations and theoretical determination of thermal conductivity and viscosity of Al_2O_3/water nanofluid, Exp. Thermal Fluid Sci. 34 (2010) 210–216.
[39] W. Duangthongsuk, S. Wongwises, Measurement of temperature-dependent thermal conductivity and viscosity of TiO_2–water nanofluids, Exp. Thermal Fluid Sci. 33 (2009) 706–714.
[40] J. Jeong, C. Li, Y. Kwon, J. Lee, S.H. Kim, R. Yun, Particle shape effect on the viscosity and thermal conductivity of ZnO nanofluids, Int. J. Refrig 36 (2013) 2233–2241.
[41] H.M. Esfe, S. Saedodin, M. Mahmoodi, Experimental studies on the convective heat transfer performance and thermophysical properties of MgO–water nanofluid under turbulent flow, Exp. Thermal Fluid Sci. 52 (2014) 68–78.
[42] D.K. Agarwal, A. Vaidyanathan, Kumar.S. Sunil, Synthesis and characterization of kerosene–alumina nanofluids, Appl. Therm. Eng. 60 (2013) 275–284.